HHS Public Access

Author manuscript

DNA Repair (Amst). Author manuscript; available in PMC 2021 June 24.

Published in final edited form as:

DNA Repair (Amst). 2017 January ; 49: 51–59. doi:10.1016/j.dnarep.2016.11.003.

Significant impact of divalent metal ions on the fidelity, sugar selectivity, and drug incorporation efficiency of human PrimPol

E. John Tokarsky[a,b], **Petra C. Wallenmeyer**[a], **Kenneth K. Phi**[a], **Zucai Suo**[*,a,b]

[a]Department of Chemistry and Biochemistry, The Ohio State University, Columbus, OH 43210, USA.

[b]The Ohio State Biophysics Program, The Ohio State University, Columbus, OH 43210, USA.

Abstract

Human PrimPol is a recently discovered bifunctional enzyme that displays DNA template-directed primase and polymerase activities. PrimPol has been implicated in nuclear and mitochondrial DNA replication fork progression and restart as well as DNA lesion bypass. Published evidence suggests that PrimPol is a Mn^{2+}-dependent enzyme as it shows significantly improved primase and polymerase activities when binding Mn^{2+}, rather than Mg^{2+}, as a divalent metal ion cofactor. Consistently, our fluorescence anisotropy assays determined that PrimPol binds to a primer/template DNA substrate with affinities of 29 and 979 nM in the presence of Mn^{2+} and Mg^{2+}, respectively. Our pre-steady-state kinetic analysis revealed that PrimPol incorporates correct dNTPs with 100-fold higher efficiency with Mn^{2+} than with Mg^{2+}. Notably, the substitution fidelity of PrimPol in the presence of Mn^{2+} was determined to be in the range of 3.4×10^{-2} to 3.8×10^{-1}, indicating that PrimPol is an error-prone polymerase. Furthermore, we kinetically determined the sugar selectivity of PrimPol to be 57–1,800 with Mn^{2+} and 150–4,500 with Mg^{2+}, and found that PrimPol was able to incorporate the triphosphates of two anticancer drugs (cytarabine and gemcitabine), but not two antiviral drugs (emtricitabine and lamivudine).

Keywords

Human PrimPol; Pre-steady-state kinetics; Enzyme regulation; Polymerase fidelity; DNA polymerase sugar selectivity

1. INTRODUCTION

Since the discovery of human PrimPol in 2013 [1; 2; 3], there has been extensive research to determine its precise role during genome replication *in vivo*. PrimPol is a bifunctional enzyme that is able to prime single-stranded DNA and subsequently catalyze primer extension via a polymerase-like, nucleotidyl transfer activity. PrimPol is only the second

[*]To whom correspondence should be addressed: 880 Biological Sciences Building, 484 W. 12th Ave., Columbus, OH 43210, USA, Telephone: (614) 688-3706; Fax: (614) 292-6773; suo.3@osu.edu.

Conflict of interest statement:
The authors declare that there are no conflicts of interest.

Supplementary data:
Supplementary figures and tables are included.

primase to be identified in humans and contains two distinct domains: an evolutionarily conserved Archaeo-Eukaryotic Primase (AEP) domain, and a UL52-like zinc finger domain that is required for its primase activity [4]. Interestingly, PrimPol is found in both the nucleus and the mitochondria and has been implicated in replication fork progression and restart, as well as DNA lesion bypass [1; 3; 5; 6]. Gene silencing of PrimPol in human cells causes profound arrest in mitochondrial DNA (mtDNA) synthesis, decreased replication fork progression rates, and increased replication protein A (RPA) foci, which is indicative of replicative stress [1; 3; 5; 7]. In PrimPol$^{-/-}$ derived mouse embryonic fibroblasts, the presence of chromosomal aberrations such as chromatid breaks [2; 3] and micronuclei [5] indicate that PrimPol is essential in the maintenance of genomic integrity. PrimPol is only the second enzyme with DNA polymerase activity to be identified in mitochondria, the other being DNA polymerase γ which is responsible for rapid and faithful mtDNA replication [8; 9]. Furthermore, PrimPol is found to play a key role in UV damage resistance, as cells lacking PrimPol have increased sensitivity to UV-C radiation [3] and GFP-tagged PrimPol was shown to be rapidly recruited to chromatin in cells treated with UV-A radiation [5]. Consistently, PrimPol can bypass common UV-induced lesions such as *cis-syn* thymine-thymine cyclobutane pyrimidine dimers and (6–4) photoproducts *in vitro* [3; 5]. PrimPol has also been shown to bypass common single-base lesions including 8-oxoguanine [6] and abasic sites [1; 5; 6]. During DNA synthesis with undamaged DNA templates, PrimPol makes one error per 10^4-10^5 nucleotide incorporations in the presence of Mg^{2+} as measured by *lacZ*, HSV-tk, and M13mp2 forward mutation assays and the errors are primarily base insertions and deletions, not substitutions [4; 10; 11]. *In vitro*, the primase and polymerase activities of PrimPol [4; 6; 11] are shown to be differentially influenced by Mg^{2+} and Mn^{2+}, the known divalent metal ion cofactors utilized by other primases and polymerases for catalysis. However, such an effect of the divalent metal ion cofactor has not been quantitatively and rigorously analyzed. To fill the void, we employed fluorescence anisotropy and pre-steady-state kinetic assays to determine the effect of the divalent metal ion cofactor on the DNA binding affinity and nucleotide incorporation efficiency of human PrimPol. In addition, we used pre-steady-state kinetics to determine the ability of human PrimPol to discriminate against ribonucleotides (rNTPs) and to incorporate the triphosphates of four nucleoside analog drugs in the presence of Mn^{2+} or Mg^{2+}.

2. Materials and Methods

2.1 Materials.

Reagents were purchased from the following companies: OptiKinase from USB corp., [γ −^{32}P]-ATP from PerkinElmer, deoxyribonucleotides (dNTPs) and rNTPs from Bioline, 2′-deoxy-2′,2′-difluorodeoxycytidine 5′-triphosphate (GemCTP) and 2′-aracytidine 5′-triphosphate (AraCTP) from TriLink BioTechnologies, 5′-triphosphate of lamivudine ((−)3TC-TP) and emtricitabine ((−)FTC-TP) from Gilead Sciences, and oligonucleotides from Integrated DNA Technologies.

2.2 Expression and Purification of Human PrimPol.

Human PrimPol containing an N-terminal 6x-histidine tag was subcloned as previously described[3], and transformed into *Escherichia coli* Rosetta (DE3) competent cells. A single

colony was used to inoculate 100 mL of LB media (30 μg/mL kanamycin and 34 μg/mL chloramphenicol) and the culture was grown at 37 °C overnight to an OD_{600} of 1.5. The starter culture was then used to inoculate 6 × 1 L of fresh LB media (30 μg/mL kanamycin and 34 μg/mL chloramphenicol) and the overexpression cultures were grown at 37 °C to an OD_{600} of 0.8 followed by rapid cooling on ice. The cultures were induced at an OD_{600} of 1.0 with 0.1 mM Isopropyl β-D-1-thiogalactopyranoside and allowed to grow at 16 °C for an additional 15 hours following induction before pelleting by centrifugation. The cell pellet was re-suspended in buffer A (50 mM Tris-HCl pH 7.5, 300 mM NaCl, 10% glycerol, 0.1% β-mercaptoethanol, 10 mM imidazole, 0.01 mM EDTA, and 0.1% IGEPAL) and supplemented with EDTA-free Protein Inhibitor Cocktail tablets (Roche) and 1 mM phenylmethanesulfonylfluoride. Cells were lysed by three passages through a French pressure cell press at 15,000 psi. The soluble fraction was isolated by ultracentrifugation at 40,000 rpm for 40 min. The cleared lysate was then incubated with charged nickel nitrilotriacetic acid (Ni-NTA) resin for 3 hr at 4 °C. The Ni-NTA beads were packed into a tricorn FPLC column and were washed with 20 column volumes (CV) of buffer A and further washed with 10 CV of 4% buffer B (buffer A containing 500 mM imidazole). Protein was eluted with a linear gradient of 4 to 100% buffer B over 15 CV and fractions were analyzed by SDS-PAGE. Protein-containing fractions were pooled and then loaded onto a HiTrap Heparin HP column (GE Healthcare). The column was washed with 5 CV buffer C (buffer A without imidazole) and then with 10 CV of 10% buffer D (buffer C containing 1 M NaCl). The protein was eluted with a gradient of 10 to 100% buffer D over 10 CV. Stepwise dialysis was performed overnight at 4°C to decrease the NaCl concentration of the eluted protein solution from 700 mM to 125 mM. The purest samples were pooled and concentrated to 500 μL using an Amicon Ultra-15 Centrifugal filter (Millipore). The protein sample was further purified in a Superdex 200 size exclusion chromatography column (GE Healthcare) to isolate full-length human PrimPol (66.5 kDa). Fractions were analyzed via SDS-PAGE and the most pure samples were pooled and dialyzed against storage buffer (50 mM Tris-HCl, pH 7.5, 400 mM NaCl, 50% glycerol, 1 mM DTT, and 0.1 mM EDTA). Using the predicted extinction coefficient (ε_{280} = 77,655 $M^{-1}cm^{-1}$), the final concentration of purified PrimPol was determined by UV-Vis spectroscopy at 280 nm and the final yield of protein was 1 mg/L of culture.

2.3 Radiolabeling and annealing DNA substrates.

All oligonucleotides were purified via PAGE and reverse-phase chromatography (Sep-Pak classic C-18 cartridges). The 21-mer primer used for the single-turnover assays was 5′-[^{32}P]-labeled by incubating it with [γ–^{32}P]-ATP and OptiKinase (USB) for 3 hr at 37 °C. The reaction was terminated by heating at 95 °C for 2 min to denature Optikinase. The radiolabeled primer was purified from any unreacted [γ–^{32}P]-ATP using a Bio-spin 6 column (Bio-Rad). The primer was then annealed to a DNA template (Table 1) in a 1:1.35 molar ratio by first heating the reaction mixture to 95 °C for 5 min and then slowly cooling the mixture to room temperature overnight.

2.4 Fluorescence anisotropy titration.

The Cy3-labeled DNA substrate 17/30-mer (Figure 1A, 30 nM) was titrated with increasing amounts of PrimPol and the anisotropy was monitored using a FluoroMax-4 (Horiba).

Assays were carried out at 25 °C in buffer E [50 mM Tris–HCl (pH = 7.5 at 25 °C), 50 mM NaCl, 0.01 mM EDTA] without divalent metal ions or in the presence of 5 mM $MnCl_2$, or 5 mM $MgCl_2$ where indicated. Excitation and emission for the Cy3 fluorophore were set to 540 and 568 nm, respectively, with a 10 nm slit width and 2 s integration time. The data obtained from anisotropy measurements were fit to Eq. 1:

$$\Delta A = (\Delta A_T/2D_0) \times \left\{ (K_{\mathrm{d,DNA}} + D_0 + E_0) - \left[(K_{\mathrm{d,DNA}} + D_0 + E_0)^2 - 4\ E_0 D_0 \right]^{1/2} \right\} \quad \text{Eq. 1}$$

Where ΔA is the change in anisotropy, ΔA_T is the maximum anisotropy change, D_0 and E_0 are the initial concentrations of DNA and PrimPol, respectively, and $K_{\mathrm{d,DNA}}$ is the equilibrium dissociation constant of the PrimPol●DNA binary complex.

2.5 Single-turnover kinetic assays.

PrimPol (300 nM) and 5′-[^{32}P]-labeled DNA (30 nM) were pre-incubated at 37 °C for 5 min in buffer E (pH = 7.5 at 37 °C) containing 5 mM DTT and 0.1 μg/ml BSA, before mixing with increasing concentrations of a single dNTP. Reaction mixtures (10 μL) were quenched with EDTA to a final concentration of 0.37 M at increasing time points. Reaction products were separated via PAGE (17% polyacrylamide, 8 M urea) and visualized using a PhosphorImager plate (Amersham Biosciences) and TyphoonTrio scanner (GE Healthcare). The product was quantified using ImageQuant software (Molecular Dynamics). The plot of product concentration versus time from each time course was fit to a single-exponential equation (Eq. 2) using non-linear regression software KaleidaGraph (Synergy Software) to determine the observed nucleotide incorporation rate constant (k_{obs}).

$$[\mathrm{Product}] = \mathrm{A}[1 - \exp(-k_{\mathrm{obs}}t)] \quad \text{Eq. 2}$$

where A is the reaction amplitude, which is equal to the initial concentration of the PrimPol●DNA binary complex. The k_{obs} values obtained from Eq. 2 were plotted against the respective concentrations of dNTP and the data were fit to a hyperbolic equation (Eq. 3):

$$k_{\mathrm{obs}} = k_{\mathrm{p}}[\mathrm{dNTP}]/([\mathrm{dNTP}] + K_{\mathrm{d}}) \quad \text{Eq. 3}$$

Where K_{d} is the apparent dissociation constant of dNTP from the PrimPol●DNA●dNTP ternary complex and k_{p} is the maximum rate constant of dNTP incorporation.

3. Results

3.1 Binding affinity of human PrimPol to DNA in the presence of Mn^{2+} or Mg^{2+}.

Human PrimPol was expressed in *Escherichia coli* and purified to >98% purity through column chromatography (Materials and Methods). To investigate the effect of divalent metal ions on the binding affinity of human PrimPol to DNA, we employed a fluorescence anisotropy assay (Materials and Methods) and determined the dissociation equilibrium constant ($K_{\mathrm{d,DNA}}$) for the PrimPol●DNA binary complex in the presence, or absence, of 5

mM $MnCl_2$ or $MgCl_2$. Similar concentrations of the divalent metal ions have been used in published studies of human PrimPol [4; 6; 11]. In the absence of any supplemental divalent metal ions, the $K_{d,DNA}$ for the binding of PrimPol to the Cy3-labeled DNA substrate 17/30-mer (Figure 1A) was measured to be 41 ± 5 nM (Figure 1B). In the presence of 5 mM Mn^{2+} or Mg^{2+}, the $K_{d,DNA}$ value was determined to be 29 ± 5 or 979 ± 119 nM, respectively (Figures 1B and 1C). Thus, the affinity ($K_{d,DNA}$ = 979 nM) of our prepared PrimPol from *E. coli* to DNA in the presence of 5 mM Mg^{2+} is ~24-fold lower than in the absence ($K_{d,DNA}$ = 41 nM) while the presence of 5 mM Mn^{2+} slightly enhanced the affinity ($K_{d,DNA}$ = 29 nM). This suggests that the presence of a molar excess of Mg^{2+} likely disrupted the interaction between the Zn^{2+} and its coordinating amino acid residues (Cys-His-Cys-Cys), which subsequently altered the binding of the zinc finger domain to the single-stranded template region in the DNA substrate [4] (Figure 1A) and weakened the overall DNA binding affinity of PrimPol (Figure 1C). Previously, similarly prepared human PrimPol to ours was found to contain Zn^{2+} in its C-terminal zinc finger domain with an occupancy of ~80% measured by using inductively coupled plasma mass spectrometry (ICP-MS) [4]. This suggests that the presence of 5 mM Mn^{2+}, a transition divalent metal ion known to bind to zinc finger motifs [12; 13], likely bound to 20% of our prepared PrimPol, which lacked Zn^{2+} based on the published ICP-MS assay results [4], and slightly improved the DNA binding affinity of our PrimPol (Figure 1B).

3.2 Correct nucleotide incorporation efficiency in the presence of Mn^{2+} or Mg^{2+}.

Besides DNA binding, Mn^{2+} and Mg^{2+} may impact the nucleotide incorporation efficiency of PrimPol differently since its AEP domain binds to divalent metal ions. To examine this possibility, single-turnover kinetic assays were performed by mixing a pre-incubated solution of PrimPol (300 nM) and 5′-[^{32}P]-labeled 21/41-mer DNA substrate D-7 (30 nM, Table 1) with increasing concentrations of correct dATP in the presence of 5 mM Mn^{2+} for various times before being quenched with 0.37 M EDTA (Materials and Methods). After the reaction products were separated and quantitated and the time courses were analyzed, we determined the maximum dATP incorporation rate constant (k_p) of 0.066 ± 0.003 s^{-1} and the apparent equilibrium dissociation constant (K_d) of 11 ± 1 μM for dATP binding (Figure 2). The substrate specificity (k_p/K_d) of dATP was then calculated to be 6.0×10^{-3} μM^{-1} s^{-1} (Table 2).

Similar single-turnover kinetic assays were performed for correct dTTP, dCTP, dGTP incorporation onto D-1, D-6, and D-8 (Table 1), respectively, and the kinetic parameters are listed in Table 2. In the presence of 5 mM Mn^{2+}, correct dNTP incorporation occurs with a k_p in the range of 0.036–0.096 s^{-1}, a K_d of 11–17 μM, and a k_p/K_d of (2.3–6.0)x10^{-3} $\mu M^{-1}s^{-1}$ (Table 2). For comparison, we performed similar single-turnover kinetic assays for a single correct dNTP incorporation onto a corresponding DNA substrate (Table 1) by PrimPol in the presence of 5 mM Mg^{2+}, *e.g.* dGTP onto D-8 (Figure S1). The kinetic data (Table 3) show that PrimPol incorporates correct dNTPs in the presence of 5 mM Mg^{2+} with a k_p of 0.011–0.020 s^{-1}, a K_d of 262–895 μM, and a k_p/K_d of (2.2–5.0)x10^{-5} $\mu M^{-1}s^{-1}$. Thus, on average, the presence of 5 mM Mg^{2+} makes PrimPol about 100-fold less efficient during correct dNTP incorporation than in the presence of 5 mM Mn^{2+} (Tables 2 and 3).

3.3 Substitution fidelity of human PrimPol in the presence of Mn^{2+} or Mg^{2+}.

To kinetically estimate the incorporation fidelity of PrimPol, we employed similar single-turnover assays to determine the pre-steady-state kinetic parameters (Table 2) for the 12 possible incorrect incorporations in the presence of 5 mM Mn^{2+}, *e.g.* dGTP incorporation opposite dT (Figure S2). Similar approaches have been used by us to determine the fidelities of other DNA polymerases [14; 15; 16; 17; 18]. The kinetic data in Table 2 demonstrate that PrimPol incorporates incorrect dNTPs in the presence of 5 mM Mn^{2+} with a k_p of 0.0024–0.035 s^{-1}, a K_d of 3–30 μM, and a k_p/K_d of (8.0×10^{-5}-2.0×10^{-3}) $\mu M^{-1}s^{-1}$. Relative to the kinetic parameters with correct dNTP incorporations (see above), incorrect dNTP incorporations occur with lower k_p and k_p/K_d values but with comparable K_d values. The substitution fidelity of PrimPol, defined as $(k_p/K_d)_{incorrect}/[(k_p/K_d)_{incorrect} + (k_p/K_d)_{correct}]$, in the presence of 5 mM Mn^{2+} is calculated to be in the range of 3.4×10^{-2} to 3.8×10^{-1} (Table 2). This fidelity indicates that PrimPol tends to make one substitution error out of every 4 to 29 nucleotide incorporations in the presence of Mn^{2+}. This substitution fidelity is about 100-fold lower than the fidelity range of 10^{-2}-10^{-4} previously estimated by Zafar *et. al.* through steady-state kinetic methods in the presence of 10 mM Mn^{2+} [6]. The large discrepancy is likely because the steady-state kinetic parameters are complicated by fast DNA product dissociation [19] and are inaccurately determined when nucleotide incorporation, *e.g.* misincorporation, is inefficient and yields little products. The low fidelity of PrimPol can be illustrated in the gel images of the time courses of incorrect dNTP incorporations, especially when multiple dCTP misincorporations occurred and even made the products longer than the template 41-mer in the presence of Mn^{2+} (Figure S3). Similar template-independent dCTP misincorporations by PrimPol have been observed previously [4; 11].

To examine if the switch from Mn^{2+} to Mg^{2+} increases the fidelity of PrimPol, we determined the kinetic parameters for individual misincorporations onto D-7 (Table 1) in the presence of 5 mM Mg^{2+}. Opposite dT, each incorrect dNTP was inefficiently incorporated and only a small amount of products were formed even after 3 hours of incubation (Figure S4C). As a result, we instead determined the k_p/K_d value, not individual k_p and K_d values, for each dNTP misincorporation and calculated the fidelity (10^{-2}-10^{-4}) of PrimPol (Table 3). Notably, the dCTP:dT misincorporation occurred with a 100-fold lower fidelity value than the other two misincorporations (Table 3). This is likely due to two consecutive dCTP incorporations onto D-7 (Table 1) with the second being a correct incorporation, while dGTP or dTTP was only misincorporated once onto D-7 (Figure S4), leading to a 100-fold difference in their k_p/K_d values (Table 3). Thus, the substitution fidelity of PrimPol in the presence of Mg^{2+} is estimated to be ~10^{-4}, which is 100–1,000 fold higher than its fidelity in the presence of Mn^{2+} (Table 2). Our fidelity value of ~10^{-4} is also comparable with the fidelity values estimated from *lacZ*, HSV-tk, and M13mp2 forward mutation assays in the presence of Mg^{2+} [4; 10; 11].

3.4 Sugar selectivity of human PrimPol in the presence of Mn^{2+} and Mg^{2+}.

Eukaryotic primases are responsible for catalyzing *de novo* primer synthesis on single-stranded DNA for the initiation of leading and lagging strand synthesis[20]. Specifically, primases utilize rNTPs to catalyze *de novo* RNA primer synthesis (7–10 bases), which can

then be extended by a specialized DNA polymerase in the presence of dNTPs to generate a hybrid 5′-RNA-DNA-3′ primer for DNA replication[21]. Contrastingly, human PrimPol prefers to utilize dNTPs for both *de novo* primer synthesis[1; 3] and subsequent primer extension[11]. Replicative polymerases can extend PrimPol-generated DNA primers during lesion bypass and replication fork restart, as there is no need for further processing of the RNA strands[22]. To quantitatively determine how much human PrimPol discriminates against rNTPs, we performed single-turnover kinetic assays (Materials and Methods) to investigate matched rNTP incorporation onto DNA/DNA substrates (Table 1) in the presence of either 5 mM $MnCl_2$ or 5 mM $MgCl_2$ (data not shown). PrimPol incorporated matched rNTPs with a range of k_p values from 0.0015–0.0092 s^{-1} and a range of K_d values of 110–744 μM, yielding calculated k_p/K_d values of 3.2×10^{-6} to 6.8×10^{-5} $\mu M^{-1}s^{-1}$ in the presence of 5 mM Mn^{2+} (Table 2). The ratio of catalytic efficiencies of correct dNTPs over matched rNTPs $[(k_p/K_d)_{dNTP}/(k_p/K_d)_{rNTP}]$ (Table 2), was calculated to give the sugar selectivity of PrimPol, which has been done similarly for other DNA polymerases [23; 24; 25; 26; 27]. The sugar selectivity of PrimPol, was found to be 57–1,800 in the presence of 5 mM Mn^{2+} (Table 2). Interestingly, both a decrease in the k_p (24-fold on average) and an increase in the K_d (30-fold on average) are responsible for rNTP discrimination by human PrimPol.

In the presence of Mg^{2+}, the individual kinetic parameters (k_p and K_d) could not be determined due to extremely slow incorporation of matched rNTPs (see above). Instead, we obtained k_{obs} values for each matched rNTP at 1 mM concentrations, and found that PrimPol incorporated matched rNTPs in the range of $(6.8–9.5)x10^{-5}$ s^{-1} (Table S2). Since the k_{obs} for correct incorporation of each dNTP at 1 mM was determined above, the ratios of observed nucleotide incorporation rate constants ($k_{obs,\ dNTP}/k_{obs,\ rNTP}$) were calculated to be in the range of 105–260 (Table S2). Thus, PrimPol incorporated correct dNTPs 150-fold (on average) more rapidly than matched rNTPs in the presence of Mg^{2+}. Although we could not determine the $K_{d,\ rNTP}/K_{d,\ dNTP}$ ratios in the presence of Mg^{2+}, we assume they are similar to the average 30-fold binding affinity ratio determined in the presence of Mn^{2+} (see above). Together, our kinetic data indicate that the sugar selectivity of human PrimPol in the presence of Mg^{2+} will be greater than 150 and could be as high as 4,500.

3.5 Incorporation efficiencies of the triphosphates of four cytidine analog drugs gemcitabine, cytarabine, emtricitabine, and lamivudine by human PrimPol.

Chain-terminating nucleoside analogs have been developed as chemotherapeutic drugs to treat cancers and antiviral drugs to combat viral infections. For example, gemcitabine (GemC) and cytarabine (AraC) have been used to treat pancreatic adenocarcinoma[28], non-muscle invasive bladder cancer[29], non-small cell lung cancer[30; 31; 32], and acute myeloid leukemia[33] while lamivudine ((−)3TC) and emtricitabine ((−)FTC) are widely prescribed drugs against human immunodeficiency virus (HIV) and Hepatitis B (HBV) infections [34; 35; 36]. The chain-terminating nucleoside analog drugs are cellularly activated into their triphosphate forms which compete against natural dNTPs for incorporation and terminate cellular and viral genomic replication once incorporated. Besides clinical efficacy, the drugs also cause various clinical toxicities and some of them have not been explained well at a molecular level. Considering human PrimPol is a recently discovered enzyme, it could incorporate the triphosphates of various nucleoside analog drugs and contribute to their

observed clinical toxicities. Here, we investigated the abilities of human PrimPol to incorporate the triphosphates of four cytidine analogs (Figure S5) by performing similar single-turnover kinetic assays (Materials and Methods) in the presence of 5 mM $MnCl_2$ or $MgCl_2$ (data not shown). The measured kinetic data are listed in Table 4. In the presence of 5 mM Mn^{2+}, AraCTP (K_d = 21 ± 4 μM) was bound by PrimPol with a similar affinity as dCTP (K_d = 16 ± 4 μM). However, the incorporation of AraCTP (k_p = 0.0057 ± 0.0004 s^{-1}) was 10-fold slower than dCTP (k_p = 0.060 ± 0.005 s^{-1}), leading to a discrimination value, calculated as $[(k_p/K_d)_{dCTP}/(k_p/K_d)_{analog}]$, of 14 (Table 4). In comparison, GemCTP was incorporated with similar k_p and K_d values as dCTP, leading to a discrimination value of 2.9 (Table 4).

In the presence of 5 mM Mg^{2+} (Tables 2–4), both AraCTP and GemCTP were incorporated by PrimPol with 2-fold lower k_p values than dCTP (Tables 3 and 4). However, the K_d values of AraCTP and dCTP are comparable while GemCTP was bound with a 5-fold higher K_d (Tables 3 and 4). The discrimination factors were calculated to be 2.1 and 9.8 for AraCTP and GemCTP, respectively (Table 4).

For (−)3TC-TP and (−)FTC-TP, the two antiviral drugs with *L*-stereochemistry, we also kinetically investigated their incorporation by human PrimPol. In the presence of 5 mM Mn^{2+}, both (−)3TC-TP and (−)FTC-TP were incorporated inefficiently and only their k_p/K_d values were determined to be 1.2×10^{-6} and 9.0×10^{-7} $\mu M^{-1}s^{-1}$, respectively (Table 4). In the presence of 5 mM Mg^{2+}, these *L*-analogs were not incorporated by PrimPol even after 3 hours at 37 °C (data not shown).

4. Discussion

4.1 Mn^{2+}, not Mg^{2+} is likely the divalent metal ion cofactor for the AEP domain of human PrimPol.

In this paper, we employed a fluorescence anisotropy assay and determined the $K_{d,DNA}$ values for the PrimPol●DNA binary complex in the presence or absence of 5 mM Mn^{2+} or Mg^{2+} (Figure 1). Strikingly, in the presence of Mg^{2+}, the affinity of PrimPol to DNA ($K_{d,DNA}$ = 979 nM) is significantly lower than other human DNA polymerases (Table S1) and the switch from Mg^{2+} to Mn^{2+} increased the DNA binding affinity ($K_{d,DNA}$ = 29 nM) of PrimPol by 34-fold. The 29 nM DNA binding affinity is likely caused by the C-terminal zinc finger domain of PrimPol which binds to the single-stranded template region in a primer/template substrate and increases the DNA binding affinity of PrimPol [4]. Since Mn^{2+} can substitute Zn^{2+} and bind to zinc finger motifs [12; 13] while Mg^{2+} cannot, the presence of a large molar excess of Mg^{2+} (5 mM) in our fluorescence anisotropy assay (Figure 1) likely disrupted the zinc finger domain of PrimPol and significantly decreased its DNA binding affinity. Furthermore, the substrate specificity (k_p/K_d) values for correct dNTP incorporations determined through pre-steady-state kinetic assays (Figure 2) are 100-fold higher with 5 mM Mn^{2+} ((2.3–6.0)x10^{-3} $\mu M^{-1}s^{-1}$, Table 2) than with 5 mM Mg^{2+} ((2.2–3.8)x10^{-5} $\mu M^{-1}s^{-1}$, Table 3). The 100-fold efficiency difference is mainly contributed by the ~48-fold dNTP binding affinity ratio since the k_p was only ~2-fold lower with Mg^{2+} versus Mn^{2+} (Tables 2 and 3). After multiplying the k_p/K_d difference by the 34-fold DNA binding affinity ratio, PrimPol is 3,400-fold less efficient as a DNA polymerase to bind and elongate

a DNA/DNA substrate in the presence of 5 mM Mg^{2+} over an equal concentration of Mn^{2+}. Considering the very low DNA and dNTP binding affinities and correct dNTP incorporation rates and efficiencies relative to other kinetically characterized human DNA polymerases in the presence of Mg^{2+} (Table S1), PrimPol is incapable of competing for access to DNA and is not efficient enough to function as a meaningful DNA polymerase during DNA replication and lesion bypass *in vivo*. For example, PrimPol is 2×10^6 fold less efficient than human DNA polymerase γ with Mg^{2+} and may not be able to play a role in mitochondrial DNA replication. However, in the presence of Mn^{2+}, PrimPol bound both DNA and dNTPs with moderately high affinities (Table 2) and incorporated correct dNTPs with comparable efficiencies as human DNA polymerases μ, κ, and ι with Mg^{2+} (Table S1). In parallel, the primase activity of PrimPol has been barely observed in the presence of 10 mM Mg^{2+} but is activated by Mn^{2+} with a concentration as low as 50 μM [1]. Together, these results suggest that the AEP domain of PrimPol likely utilizes Mn^{2+}, not Mg^{2+}, as divalent metal ion cofactor in order to carry out both polymerase and primase activities *in vivo*. Recently, Polymerase Delta Interacting Protein 2 (PolDIP2) has been shown to interact with the AEP domain and moderately enhance the DNA binding affinity and polymerase processivity of human PrimPol in the presence of Mg^{2+} [37]. If the enhancement is also true in the presence of Mn^{2+}, the combined favorable effect of PolDIP2 and Mn^{2+} will further solidify the role of PrimPol as a legitimate bifunctional enzyme in replication fork progression and restart, as well as DNA lesion bypass [1; 3; 5; 6]. More studies, especially structural investigation, are needed to verify the modulation effect of both PolDIP2 and Mn^{2+} on the structure and function of PrimPol.

Interestingly, some of the thermodynamic and kinetic parameters reported here are different than those reported by Mislak and Anderson (*Antimicrob. Agents Chemother.* **60**, 561–569) in 2016 [38]. Specifically, their reported $K_{d,\mathrm{DNA}}$ values [38], measured by electrophoretic mobility shift assays (EMSAs), are larger than ours by 11- to 25-fold in the presence of Mn^{2+} and 8-fold in the presence of Mg^{2+}. The relative enhancement in the DNA binding affinities by switching from Mg^{2+} ($K_{d,\mathrm{DNA}}$ = 340–720 nM) to Mn^{2+} ($K_{d,\mathrm{DNA}}$ = 8 μM) in their studies [38] is comparable to the 34-fold DNA binding affinity enhancement reported here. The large discrepancy between our and their $K_{d,\mathrm{DNA}}$ values is likely due to the different methods used the two studies. The EMSAs employed by Mislak and Anderson [38] are not performed under true equilibrium conditions and can only be used to estimate the $K_{d,\mathrm{DNA}}$ values. In comparison, our fluorescence anisotropy assays are a superior method because the protein and DNA binding and dissociation were allowed to come to equilibrium in solution, and polarization was measured promptly after equilibrium was achieved. Furthermore, the sole variable to affect equilibrium in an fluorescence anisotropy assay is the concentration of DNA or PrimPol in their binding interactions while the gel matrix and electrical current can perturb the protein-DNA complex formation in an EMSA. Likewise, the slightly lower k_p and k_p/K_d values measured here may have been caused by differences in the reaction buffers used in our single-turnover assays (Materials and Methods) and those used by Mislak and Anderson (10 mM Bis-Tris propane, pH = 7.0, 1 mM DTT, 10 mM $MnCl_2$) [38]. Furthermore, the slow single-turnover rates (Tables 2 and 3) measured here are comparable to the steady-state rates reported by Zafar *et al.*[6] Therefore, we expect not to observe an initial burst of product formation under pre-steady-state kinetic conditions in

which the DNA substrate is only a few fold molar excess over the enzyme. Additionally, it should be noted that PrimPol is an atypical DNA polymerase and its kinetic mechanism is likely to be different from those of canonical polymerases. Thus, the assignments of the steady-state and pre-steady state rates within the mechanism of polymerization catalyzed by PrimPol remain to be established.

4.2 The polymerase activity of human PrimPol is error-prone in the presence of Mn^{2+}.

The substitution fidelity of PrimPol was kinetically determined to be in the range of 3.4×10^{-2} to 3.8×10^{-1} in the presence of Mn^{2+} (Table 2). Thus, PrimPol poorly discriminated against incorrect dNTPs during primer elongation. The fidelity of PrimPol is actually comparable to the low fidelities of human Y-family DNA polymerases which bypass DNA lesions *in vivo* [39]. PrimPol incorporated an incorrect dNTP with only 2- to 23-fold slower k_p than a correct dNTP and bound to all dNTPs with comparable affinities (K_d = 3–30 μM), demonstrating a kinetic basis for the low fidelity of PrimPol. These data also indicate that incorrect dNTPs are strong competitive inhibitors against correct dNTPs during polymerization in the presence of Mn^{2+}. Although significantly less efficient, PrimPol has a fidelity of 10^{-4} in the presence of Mg^{2+} (Table 3) which is 100–1,000 fold more faithful than in the presence of Mn^{2+} (Table 2). Consistently, the switch from Mg^{2+} to Mn^{2+} as the divalent metal ion cofactor is known to increase misincorporation frequency for many DNA polymerases and can lead to increased genomic instability [40; 41; 42; 43; 44].

4.3 Human PrimPol displays moderate sugar selectivity in the presence of Mn^{2+} and Mg^{2+}.

Human PrimPol has been shown to select dNTPs over rNTPs during primer extension with both DNA and RNA primers [11]. Consistently, our kinetic studies quantitatively estimated the sugar selectivity of PrimPol to be 57–1,800 in the presence of Mn^{2+} (Table 2) and 150–4,500 in the presence of Mg^{2+} (see 3.4 in Results). Thus, human PrimPol displays a modest sugar selectivity (740 on average with Mn^{2+}) [45], which is comparable to the sugar selectivities of human DNA polymerases α (500), γ (1,000) and Rev1 (280), measured using similar kinetic methods[31; 45; 46]. Interestingly, a very recently published crystal structure of the AEP domain of human PrimPol in complex with DNA and an incoming dATP [47] was modeled with an rATP to replace the dATP in the enzyme active site. Notably, the 2′ hydroxyl of the rATP ribose sterically clashed with the backbone carbonyl of Asn289. Thus, the 67-fold difference between the K_d values of correct dATP and matched rATP in the presence of Mn^{2+} (Table 1) likely arises from the clash between the rATP and the steric gate residue Asn289 [45], similar to what has been observed with other DNA polymerases [30; 31; 32; 44; 45], *e.g.* rNTP with Tyr12 in *Sulfolobus solfataricus* DNA polymerase IV (Dpo4) [48; 49]. Furthermore, since the AEP domain of PrimPol contains a single active site that catalyzes both primase and polymerase activities[1; 2; 3], the same mode of sugar selection is likely utilized by both the primase and polymerase activities of PrimPol. Our ongoing structural and mutagenic studies of PrimPol will further characterize the steric gate residue in this bifunctional enzyme.

4.4 Human PrimPol was able to incorporate the triphosphates of gemcitabine and cytarabine, but not emtricitabine and lamivudine.

Nucleoside Reverse Transcriptase Inhibitors (NRTIs) specifically target the active site of RTs and halt viral genomic replication. Mitochondrial toxicity of NRTIs has been associated with the incorporation of the triphosphates of NRTIs by human DNA polymerase γ, a main off-target issue. Based on the existence of PrimPol in the mitochondria, it is possible that PrimPol could potentially incorporate NRTIs and contribute to their mitochondrial toxicology. Recently, human PrimPol has been shown to incorporate the triphosphates of anti-HIV NRTI drugs zidovudine and abacavir [38] and re-prime downstream from NRTI-terminated DNA primers [50]. In this paper, we found that human PrimPol incorporated the triphosphates of antiviral drugs emtricitabine ((−)3TC-TP) and lamivudine ((−)FTC-TP) with extremely low efficiencies (10^{-6} to 10^{-7} μM^{-1} s^{-1}) in the presence of Mn^{2+} (Table 4) but did not incorporate them even after 3 hours in the presence of Mg^{2+} at 37 °C. Since (−)3TC-TP and (−)FTC-TP, unlike natural dNTPs, possess *L*-stereochemistry (Figure S5), our results suggest that PrimPol, like Dpo4[51] and human DNA polymerase λ[36], possesses strong *D*-stereoselectivity. Our results further suggest that human PrimPol is an unlikely off-target of these two drugs *in vivo*.

In comparison, human PrimPol incorporated AraCTP, GemCTP, and dCTP, which possess *D*-stereochemistry (Figure S5), with comparable k_p/K_d values in the presence of Mn^{2+} or Mg^{2+}, leading to the discrimination factors in the range of 2–14 (Table 4). It suggests that the inhibition of PrimPol by these anticancer chain-terminating nucleotide analogs likely contributes to their clinical toxicities. Interestingly, there is an order for the K_d values: dCTP < AraCTP < GemCTP < rCTP (Tables 2–4). This order is closely correlated to the size of the 2′-group oriented below the sugar ring, likely due to its clash with an unidentified steric gate residue in PrimPol (see above). As the size of the 2′-group increases, the K_d value increases simultaneously. Specifically, the 2′-group is a small hydrogen atom in both dCTP and AraCTP, a medium sized fluorine atom in GemCTP, and a comparatively larger sized hydroxyl group in rCTP (Figure S5), which leads to the above K_d order. The slightly larger K_d value of AraCTP over dCTP may be contributed by the size difference between their 2′-groups oriented above the sugar ring.

In summary, our fluorescence anisotropy and pre-steady-state kinetic studies demonstrate that human PrimPol is a moderately efficient and highly unfaithful DNA polymerase in the presence of Mn^{2+} but is too inefficient to function as a DNA polymerase in the presence of Mg^{2+}. Human PrimPol possesses modest sugar selectivity and can incorporate the triphosphates of anticancer gemcitabine and cytarabine, but not antiviral emtricitabine and lamivudine.

Supplementary Material

Refer to Web version on PubMed Central for supplementary material.

Acknowledgements:

The authors are grateful to Dr. Aiden Doherty for kindly providing us with the plasmid encoding wild-type human PrimPol, and Dr. Joy Feng (Gilead Sciences, Inc.) for providing (−)FTC-TP and (−)3TC-TP. We would also like to thank Walter Zahurancik for helpful editing of this manuscript.

Funding:

This work was supported by National Institutes of Health [grants ES026821, ES024585, and ES009127] to Z.S.

Abbreviations:

1

(−)3TC	(−)-β-*L*-2′−3′-dideoxy-3′-thiacytidine
(−)3TC-TP	5′-triphosphate of (−)3TC or lamivudine
(−)FTC	(−)-β -*L*-2′−3′-dideoxy-5-fluoro-3′-thiacytidine
(−)FTC-TP	5′-triphosphate of (−)FTC or emtricitabine
AEP	Archaeo-Eukaryotic Primase
dNTP	deoxyribonucleotide
AraCTP	2′-aracytidine-5′-triphosphate
Dpo4	DNA polymerase IV
GemCTP	2′-deoxy-2′,2′-difluorodeoxycytidine-5′-triphosphate
mtDNA	mitochondrial DNA
NRTI	Nucleoside Reverse Transcriptase Inhibitor
PolDIP2	Polymerase Delta Interacting Protein 2
ICP-MS	inductively coupled plasma mass spectrometry
RPA	replication protein A
rNTP	ribonucleotide

References

1. Garcia-Gomez S, Reyes A, Martinez-Jimenez MI, Chocron ES, Mouron S, Terrados G, Powell C, Salido E, Mendez J, Holt IJ & Blanco L (2013). PrimPol, an archaic primase/polymerase operating in human cells. Mol Cell 52, 541–53. [PubMed: 24207056]
2. Wan L, Lou J, Xia Y, Su B, Liu T, Cui J, Sun Y, Lou H & Huang J (2013). hPrimpol1/CCDC111 is a human DNA primase-polymerase required for the maintenance of genome integrity. EMBO Rep 14, 1104–12. [PubMed: 24126761]
3. Bianchi J, Rudd SG, Jozwiakowski SK, Bailey LJ, Soura V, Taylor E, Stevanovic I, Green AJ, Stracker TH, Lindsay HD & Doherty AJ (2013). PrimPol bypasses UV photoproducts during eukaryotic chromosomal DNA replication. Mol Cell 52, 566–73. [PubMed: 24267451]

4. Keen BA, Jozwiakowski SK, Bailey LJ, Bianchi J & Doherty AJ (2014). Molecular dissection of the domain architecture and catalytic activities of human PrimPol. Nucleic Acids Res 42, 5830–45. [PubMed: 24682820]
5. Mouron S, Rodriguez-Acebes S, Martinez-Jimenez MI, Garcia-Gomez S, Chocron S, Blanco L & Mendez J (2013). Repriming of DNA synthesis at stalled replication forks by human PrimPol. Nat Struct Mol Biol 20, 1383–9. [PubMed: 24240614]
6. Zafar MK, Ketkar A, Lodeiro MF, Cameron CE & Eoff RL (2014). Kinetic analysis of human PrimPol DNA polymerase activity reveals a generally error-prone enzyme capable of accurately bypassing 7,8-dihydro-8-oxo-2'-deoxyguanosine. Biochemistry 53, 6584–94. [PubMed: 25255211]
7. Balajee AS & Geard CR (2004). Replication protein A and gamma-H2AX foci assembly is triggered by cellular response to DNA double-strand breaks. Exp Cell Res 300, 320–34. [PubMed: 15474997]
8. Lee HR & Johnson KA (2006). Fidelity of the human mitochondrial DNA polymerase. J Biol Chem 281, 36236–40. [PubMed: 17005554]
9. Graves SW, Johnson AA & Johnson KA (1998). Expression, purification, and initial kinetic characterization of the large subunit of the human mitochondrial DNA polymerase. Biochemistry 37, 6050–8. [PubMed: 9558343]
10. Guilliam TA, Jozwiakowski SK, Ehlinger A, Barnes RP, Rudd SG, Bailey LJ, Skehel JM, Eckert KA, Chazin WJ & Doherty AJ (2015). Human PrimPol is a highly error-prone polymerase regulated by single-stranded DNA binding proteins. Nucleic Acids Res 43, 1056–68. [PubMed: 25550423]
11. Martinez-Jimenez MI, Garcia-Gomez S, Bebenek K, Sastre-Moreno G, Calvo PA, Diaz-Talavera A, Kunkel TA & Blanco L (2015). Alternative solutions and new scenarios for translesion DNA synthesis by human PrimPol. DNA Repair (Amst) 29, 127–38. [PubMed: 25746449]
12. Berg JM (1990). Zinc fingers and other metal-binding domains. Elements for interactions between macromolecules. J Biol Chem 265, 6513–6. [PubMed: 2108957]
13. Thiesen HJ & Bach C (1991). Transition metals modulate DNA-protein interactions of SP1 zinc finger domains with its cognate target site. Biochem Biophys Res Commun 176, 551–7. [PubMed: 2025269]
14. Fiala KA & Suo Z (2004). Pre-Steady-State Kinetic Studies of the Fidelity of Sulfolobus solfataricus P2 DNA Polymerase IV. Biochemistry 43, 2106–15. [PubMed: 14967050]
15. Zhang L, Brown JA, Newmister SA & Suo Z (2009). Polymerization fidelity of a replicative DNA polymerase from the hyperthermophilic archaeon Sulfolobus solfataricus P2. Biochemistry 48, 7492–501. [PubMed: 19456141]
16. Zahurancik WJ, Klein SJ & Suo Z (2014). Significant contribution of the 3'-->5' exonuclease activity to the high fidelity of nucleotide incorporation catalyzed by human DNA polymerase. Nucleic Acids Res 42, 13853–60. [PubMed: 25414327]
17. Fiala KA, Abdel-Gawad W & Suo Z (2004). Pre-Steady-State Kinetic Studies of the Fidelity and Mechanism of Polymerization Catalyzed by Truncated Human DNA Polymerase lambda. Biochemistry 43, 6751–62. [PubMed: 15157109]
18. Roettger MP, Fiala KA, Sompalli S, Dong Y & Suo Z (2004). Pre-steady-state kinetic studies of the fidelity of human DNA polymerase mu. Biochemistry 43, 13827–38. [PubMed: 15504045]
19. Johnson KA (1995). Rapid quench kinetic analysis of polymerases, adenosinetriphosphatases, and enzyme intermediates. Methods Enzymol 249, 38–61. [PubMed: 7791620]
20. Georgescu RE, Schauer GD, Yao NY, Langston LD, Yurieva O, Zhang D, Finkelstein J & O'Donnell ME (2015). Reconstitution of a eukaryotic replisome reveals suppression mechanisms that define leading/lagging strand operation. Elife 4, e04988. [PubMed: 25871847]
21. Zerbe LK & Kuchta RD (2002). The p58 subunit of human DNA primase is important for primer initiation, elongation, and counting. Biochemistry 41, 4891–900. [PubMed: 11939784]
22. Guilliam TA, Keen BA, Brissett NC & Doherty AJ (2015). Primase-polymerases are a functionally diverse superfamily of replication and repair enzymes. Nucleic Acids Res 43, 6651–64. [PubMed: 26109351]

23. Brown JA, Fiala KA, Fowler JD, Sherrer SM, Newmister SA, Duym WW & Suo Z (2010). A novel mechanism of sugar selection utilized by a human X-family DNA polymerase. J Mol Biol 395, 282–90. [PubMed: 19900463]
24. Astatke M, Ng K, Grindley ND & Joyce CM (1998). A single side chain prevents Escherichia coli DNA polymerase I (Klenow fragment) from incorporating ribonucleotides. Proc Natl Acad Sci U S A 95, 3402–7. [PubMed: 9520378]
25. Yang G, Franklin M, Li J, Lin TC & Konigsberg W (2002). A conserved Tyr residue is required for sugar selectivity in a Pol alpha DNA polymerase. Biochemistry 41, 10256–61. [PubMed: 12162740]
26. Nick McElhinny SA & Ramsden DA (2003). Polymerase mu is a DNA-directed DNA/RNA polymerase. Mol Cell Biol 23, 2309–15. [PubMed: 12640116]
27. Boule JB, Rougeon F & Papanicolaou C (2001). Terminal deoxynucleotidyl transferase indiscriminately incorporates ribonucleotides and deoxyribonucleotides. J Biol Chem 276, 31388–93. [PubMed: 11406636]
28. Burris HA 3rd, Moore MJ, Andersen J, Green MR, Rothenberg ML, Modiano MR, Cripps MC, Portenoy RK, Storniolo AM, Tarassoff P, Nelson R, Dorr FA, Stephens CD & Von Hoff DD (1997). Improvements in survival and clinical benefit with gemcitabine as first-line therapy for patients with advanced pancreas cancer: a randomized trial. J Clin Oncol 15, 2403–13. [PubMed: 9196156]
29. Shelley MD, Jones G, Cleves A, Wilt TJ, Mason MD & Kynaston HG (2012). Intravesical gemcitabine therapy for non-muscle invasive bladder cancer (NMIBC): a systematic review. BJU Int 109, 496–505. [PubMed: 22313502]
30. Kroep JR, Giaccone G, Tolis C, Voorn DA, Loves WJ, Groeningen CJ, Pinedo HM & Peters GJ (2000). Sequence dependent effect of paclitaxel on gemcitabine metabolism in relation to cell cycle and cytotoxicity in non-small-cell lung cancer cell lines. Br J Cancer 83, 1069–76. [PubMed: 10993656]
31. Brown JA, Fowler JD & Suo Z (2010). Kinetic basis of nucleotide selection employed by a protein template-dependent DNA polymerase. Biochemistry 49, 5504–10. [PubMed: 20518555]
32. Fowler JD, Brown JA, Johnson KA & Suo Z (2008). Kinetic investigation of the inhibitory effect of gemcitabine on DNA polymerization catalyzed by human mitochondrial DNA polymerase. J Biol Chem 283, 15339–48. [PubMed: 18378680]
33. Liu Yin JA, Johnson PR, Davies JM, Flanagan NG, Gorst DW & Lewis MJ (1991). Mitozantrone and cytosine arabinoside as first-line therapy in elderly patients with acute myeloid leukaemia. Br J Haematol 79, 415–20. [PubMed: 1751369]
34. Brown JA, Pack LR, Fowler JD & Suo Z (2011). Pre-steady-state kinetic analysis of the incorporation of anti-HIV nucleotide analogs catalyzed by human X- and Y-family DNA polymerases. Antimicrob Agents Chemother 55, 276–83. [PubMed: 21078938]
35. Brown JA, Pack LR, Fowler JD & Suo Z (2012). Presteady state kinetic investigation of the incorporation of anti-hepatitis B nucleotide analogues catalyzed by noncanonical human DNA polymerases. Chem Res Toxicol 25, 225–33. [PubMed: 22132702]
36. Vyas R, Zahurancik WJ & Suo Z (2014). Structural basis for the binding and incorporation of nucleotide analogs with L-stereochemistry by human DNA polymerase lambda. Proc Natl Acad Sci U S A 111, E3033–42. [PubMed: 25015085]
37. Guilliam TA, Bailey LJ, Brissett NC & Doherty AJ (2016). PolDIP2 interacts with human PrimPol and enhances its DNA polymerase activities. Nucleic Acids Res 44, 3317–29. [PubMed: 26984527]
38. Mislak AC & Anderson KS (2016). Insights into the Molecular Mechanism of Polymerization and Nucleoside Reverse Transcriptase Inhibitor Incorporation by Human PrimPol. Antimicrob Agents Chemother 60, 561–9. [PubMed: 26552983]
39. Maxwell BA & Suo Z (2014). Recent insight into the kinetic mechanisms and conformational dynamics of Y-Family DNA polymerases. Biochemistry 53, 2804–14. [PubMed: 24716482]
40. Pelletier H, Sawaya MR, Wolfle W, Wilson SH & Kraut J (1996). A structural basis for metal ion mutagenicity and nucleotide selectivity in human DNA polymerase beta. Biochemistry 35, 12762–77. [PubMed: 8841119]

41. Beckman RA, Mildvan AS & Loeb LA (1985). On the fidelity of DNA replication: manganese mutagenesis in vitro. Biochemistry 24, 5810–7. [PubMed: 3910084]
42. El-Deiry WS, Downey KM & So AG (1984). Molecular mechanisms of manganese mutagenesis. Proc Natl Acad Sci U S A 81, 7378–82. [PubMed: 6095289]
43. Goodman MF, Keener S, Guidotti S & Branscomb EW (1983). On the enzymatic basis for mutagenesis by manganese. J Biol Chem 258, 3469–75. [PubMed: 6833210]
44. Loeb LA & Kunkel TA (1982). Fidelity of DNA synthesis. Annu Rev Biochem 51, 429–57. [PubMed: 6214209]
45. Richardson FC, Kuchta RD, Mazurkiewicz A & Richardson KA (2000). Polymerization of 2'-fluoro- and 2'-O-methyl-dNTPs by human DNA polymerase alpha, polymerase gamma, and primase. Biochem Pharmacol 59, 1045–52. [PubMed: 10704933]
46. Brown JA & Suo Z (2011). Unlocking the sugar "steric gate" of DNA polymerases. Biochemistry 50, 1135–42. [PubMed: 21226515]
47. Rechkoblit O, Gupta YK, Malik R, Rajashankar KR, Johnson RE, Prakash L, Prakash S & Aggarwal AK (2016). Structure and mechanism of human PrimPol, a DNA polymerase with primase activity. Sci Adv 2, e1601317.
48. Sherrer SM, Beyer DC, Xia CX, Fowler JD & Suo Z (2010). Kinetic Basis of Sugar Selection by a Y-Family DNA Polymerase from Sulfolobus solfataricus P2. Biochemistry 49, 10179–10186. [PubMed: 20973506]
49. Kirouac KN, Suo Z & Ling H (2011). Structural mechanism of ribonucleotide discrimination by a Y-family DNA polymerase. J Mol Biol 407, 382–90. [PubMed: 21295588]
50. Kobayashi K, Guilliam TA, Tsuda M, Yamamoto J, Bailey LJ, Iwai S, Takeda S, Doherty AJ & Hirota K (2016). Repriming by PrimPol is critical for DNA replication restart downstream of lesions and chain-terminating nucleosides. Cell Cycle 15, 1997–2008. [PubMed: 27230014]
51. Gaur V, Vyas R, Fowler JD, Efthimiopoulos G, Feng JY & Suo Z (2014). Structural and kinetic insights into binding and incorporation of L-nucleotide analogs by a Y-family DNA polymerase. Nucleic Acids Res 42, 9984–95. [PubMed: 25104018]

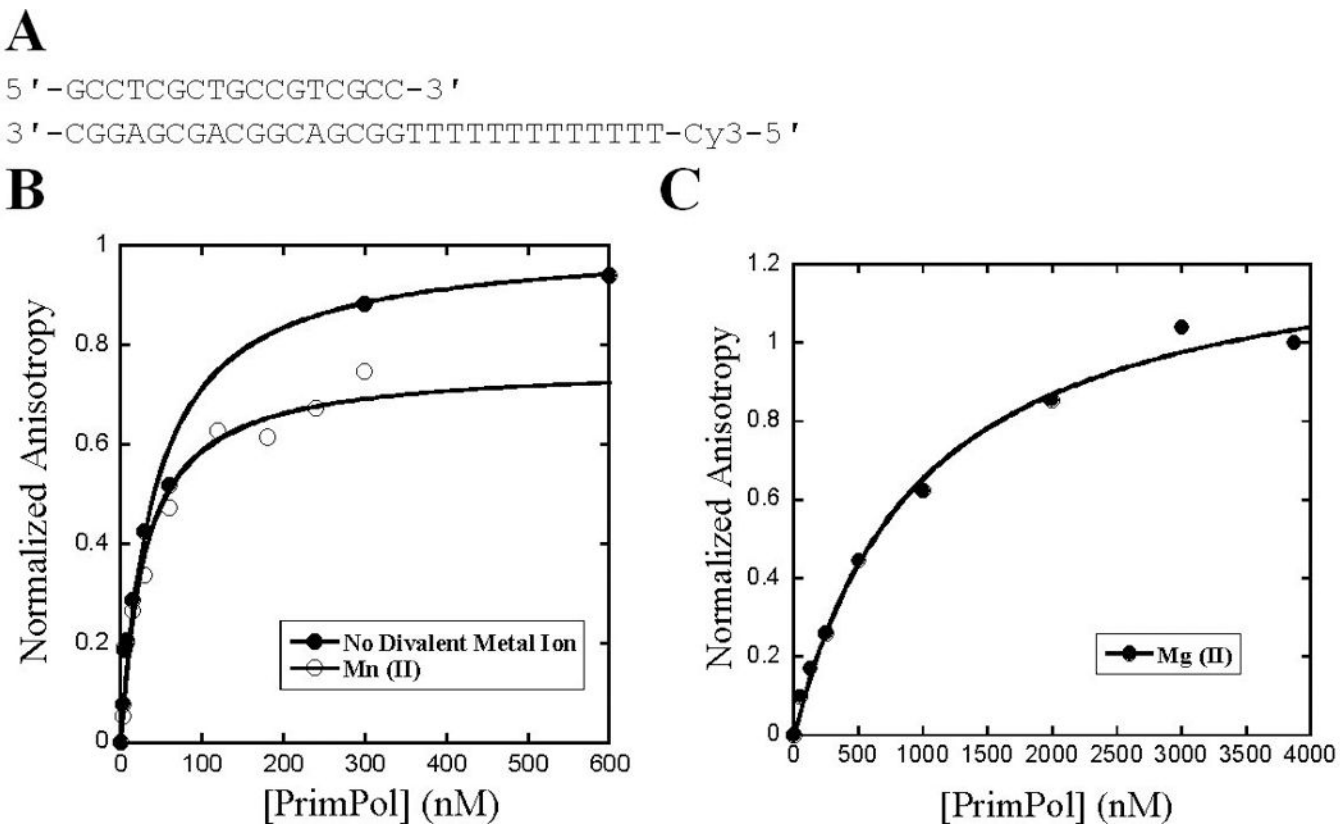

FIGURE 1.

Determination of the binding affinity of PrimPol to DNA in the presence or absence of a divalent metal ion. (A) Cy3-labeled DNA 17/30-mer. Increasing amounts of PrimPol were titrated into a fixed concentration of Cy3-labeled 17/30-mer (30 nM). The plot of the concentration of the binary complex PrimPol●DNA *versus* the concentration of PrimPol was fit to Eq. 1 (Materials and Methods) to obtain $K_{d,DNA}$. The $K_{d,DNA}$ value was 41 ± 5 nM in the absence of any divalent metal ions (B), 29 ± 5 nM in the presence of 5 mM $MnCl_2$ (B), 979 ± 119 nM in the presence of 5 mM $MgCl_2$ (C).

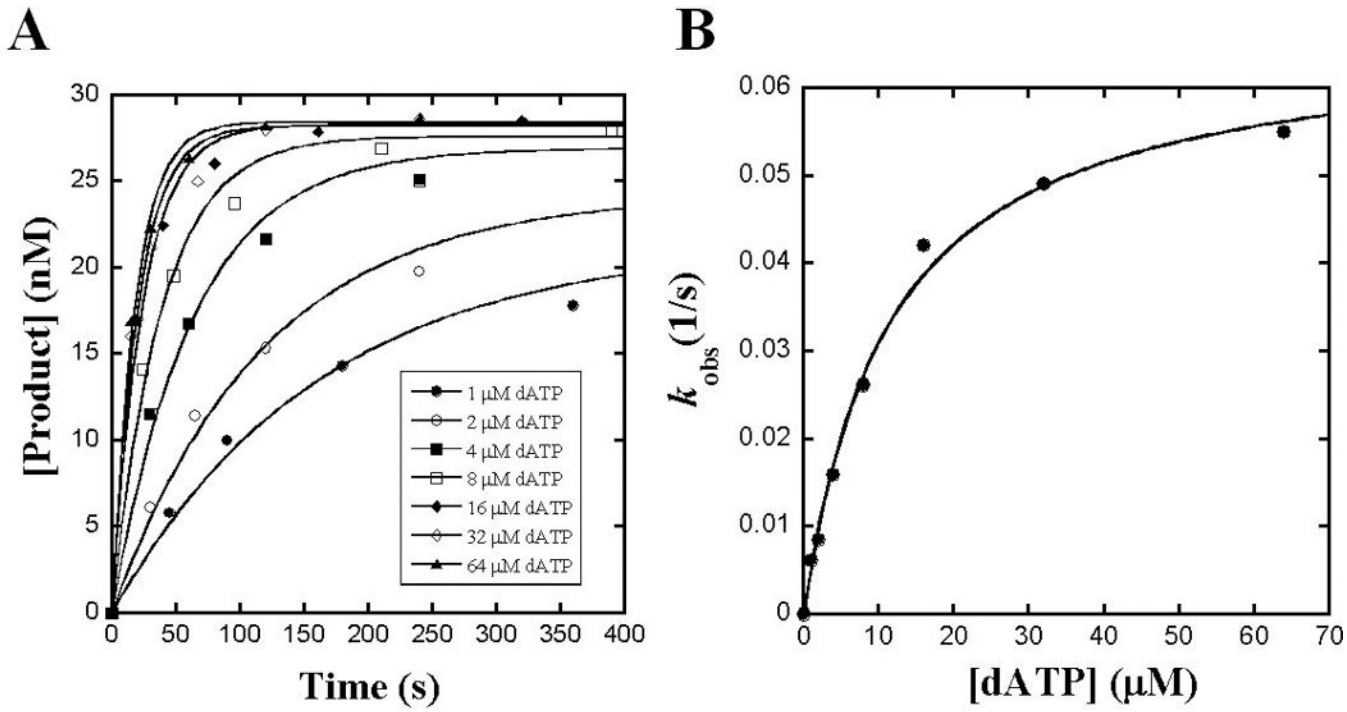

FIGURE 2.

Determination of kinetic parameters for dATP incorporation opposite dT in the presence of Mn^{2+} at 37 °C. (A) A pre-incubated solution of PrimPol (300 nM) and D-7 DNA substrate (30 nM, Table 1) was mixed with increasing concentrations of dATP in the presence of 5 mM Mn^{2+} at 37 °C. The product concentrations were plotted against reaction times and each time course was fit to Eq. 2 (Materials and Methods) to yield k_{obs}. (B) The k_{obs} values were plotted against respective concentrations of dATP and the plot was fit to Eq. 3 (Materials and Methods) to yield a k_p of 0.066 ± 0.003 s^{-1} and a K_d of 11 ± 1 μM.

Table 1.

21/41-mer DNA substrates

D-1
5′-CGCAGCCGTCCAACCAACTCA-3′
3′-GCGTCGGCAGGTTGGTTGAGTAGCAGCTAGGTTACGGCAGG-5′
D-6
5′-CGCAGCCGTCCAACCAACTCA-3′
3′-GCGTCGGCAGGTTGGTTGAGTGGCAGCTAGGTTACGGCAGG-5′
D-7
5′-CGCAGCCGTCCAACCAACTCA-3′
3′-GCGTCGGCAGGTTGGTTGAGTTGCAGCTAGGTTACGGCAGG-5′
D-8
5′-CGCAGCCGTCCAACCAACTCA-3′
3′-GCGTCGGCAGGTTGGTTGAGTCGCAGCTAGGTTACGGCAGG-5′

TABLE 2.

Pre-steady-state kinetic parameters for nucleotide incorporation onto 21/41-mer DNA substrates catalyzed by PrimPol in the presence of 5 mM Mn^{2+} at 37 °C.

dNTP	k_p (s^{-1})	K_d (μM)	k_p/K_d ($\mu M^{-1}\ s^{-1}$)	Fidelity[a]	Sugar Selectivity[b]
D-1 (Template dA)					
dTTP	0.096 ± 0.004	17 ± 2	5.8×10^{-3}	-	
dATP	0.0083 ± 0.0001	4.1 ± 0.3	2.0×10^{-3}	2.6×10^{-1}	
dCTP	0.014 ± 0.0009	13 ± 4	1.1×10^{-3}	1.7×10^{-1}	
dGTP	0.0047 ± 0.0007	13 ± 4	3.6×10^{-4}	6.0×10^{-2}	
rUTP	0.0018 ± 0.0002	561 ± 160	3.2×10^{-6}	5.5×10^{-4}	1800
D-6 (Template dG)					
dCTP	0.060 ± 0.005	16 ± 4	3.8×10^{-3}	-	
dATP	0.011 ± 0.00005	20 ± 3	5.5×10^{-4}	1.3×10^{-1}	
dGTP	0.035 ± 0.003	27 ± 8	1.3×10^{-3}	2.6×10^{-1}	
dTTP	0.0058 ± 0.0005	14 ± 6	4.2×10^{-4}	9.9×10^{-2}	
rCTP	0.0092 ± 0.0002	136 ± 7	6.7×10^{-5}	1.7×10^{-2}	57
D-7 (Template dT)					
dATP	0.066 ± 0.003	11 ± 1	6.0×10^{-3}	-	
dCTP	0.013 ± 0.002	17 ± 9	7.6×10^{-4}	1.1×10^{-1}	
dGTP	0.017 ± 0.001	22 ± 4	7.7×10^{-4}	1.1×10^{-1}	
dTTP	0.0029 ± 0.0002	3 ± 1	1.0×10^{-3}	1.4×10^{-1}	
rATP	0.0047 ± 0.0006	744 ± 234	6.3×10^{-6}	1.0×10^{-3}	950
D-8 (Template dC)					
dGTP	0.036 ± 0.002	16 ± 3	2.3×10^{-3}	-	
dATP	0.0049 ± 0.0003	16 ± 3	3.0×10^{-4}	1.2×10^{-1}	
dCTP	0.014 ± 0.001	10 ± 3	1.4×10^{-3}	3.8×10^{-1}	
dTTP	0.0024 ± 0.0004	30 ± 7	8.0×10^{-5}	3.4×10^{-2}	
rGTP	0.0015 ± 0.0001	110 ± 29	1.4×10^{-5}	6.1×10^{-3}	160

[a] Calculated as $(k_p/K_d)_{incorrect}/[(k_p/K_d)_{correct} + (k_p/K_d)_{incorrect}]$

[b] Calculated as $(k_p/K_d)_{dNTP}/(k_p/K_d)_{rNTP}$

TABLE 3.

Pre-steady-state kinetic parameters for dNTP incorporation onto 21/41-mer DNA substrates catalyzed by PrimPol in the presence of 5 mM Mg^{2+} at 37 °C.

dNTP	k_p (s^{-1})	K_d (μM)	k_p/K_d ($\mu M^{-1}\ s^{-1}$)	Fidelity[a]
D-1 (Template dA)				
dTTP	0.020 ± 0.002	526 ± 99	3.8×10^{-5}	
D-6 (Template dG)				
dCTP	0.013 ± 0.0008	262 ± 55	5.0×10^{-5}	
D-7 (Template dT)				
dATP	0.011 ± 0.0007	388 ± 65	2.8×10^{-5}	-
dCTP	Not determined	Not determined	3.1×10^{-7}	1.1×10^{-2}
dGTP	Not determined	Not determined	1.3×10^{-8}	4.6×10^{-4}
dTTP	Not determined	Not determined	1.7×10^{-8}	6.1×10^{-4}
D-8 (Template dC)				
dGTP	0.020 ± 0.0006	895 ± 60	2.2×10^{-5}	

[a] Calculated as $(k_p/K_d)_{incorrect}/[(k_p/K_d)_{correct} + (k_p/K_d)_{incorrect}]$

TABLE 4.

Pre-steady-state kinetic parameters for incorporation of dCTP analogs onto D-6 (Table 1) catalyzed by human PrimPol at 37 °C.

NTP	k_p (s^{-1})	K_d (μM)	k_p/K_d ($\mu M^{-1}\ s^{-1}$)	Discrimination[a]
In the presence of 5 mM Mn^{2+}				
AraCTP	0.0057 ± 0.0004	21 ± 4	2.7×10^{-4}	14
GemCTP	0.058 ± 0.0006	45 ± 2	1.3×10^{-3}	2.9
(−)3TC-TP	Not determined	Not determined	1.2×10^{-6}	3,200
(−)FTC-TP	Not determined	Not determined	9.0×10^{-7}	4,200
In the presence of 5 mM Mg^{2+}				
AraCTP	0.0076 ± 0.0003	316 ± 44	2.4×10^{-5}	2.1
GemCTP	0.0071 ± 0.0006	1,380 ± 255	5.1×10^{-6}	9.8
(−)3TC-TP	No observed incorporation			
(−)FTC-TP	No observed incorporation			

[a] Calculated as $(k_p/K_d)_{dCTP}/(k_p/K_d)_{analog}$ with the $(k_p/K_d)_{dCTP}$ values from Tables 2 and 3.